Technologies and Materials for Renewable Energy, Environment & Sustainability

Performance of R.C. Flat Slabs with Normal and Reactive Powder Concrete Drop Panel

AIPCP25-CF-TMREES2025-00082 | Article

Performance of R.C. Flat Slabs with Normal and Reactive Powder Concrete Drop Panel

Alaa Nozad Faeq [1,a)] and Ali I. Salahaldin [1,b)]

[1] University of Kirkuk, College of Engineering, Civil Engineering Department, Iraq.

[a)] Corresponding author: alaa.n.faeq@gmail.com
[b)] ali.ihsan@uokirkuk.edu.iq

Abstract. Previous studies have shown that flat slabs constructed from reactive powder concrete (RPC) exhibit greater punching shear strength compared to those made from normal concrete (NC). However, constructing a complete slab using RPC may not be economically viable. This study aimed to determine the optimal use of RPC in the critical punching shear area, while the rest of the slab remains composed of NC. Four flat slab specimens with dimensions (940×940×60 mm) and drop panels (500×500×30 mm) were tested, with two column sizes (75×75 mm, 125×125 mm) and two types of concrete within the drop panel area (normal concrete and RPC). The slabs were examined under concentric loading to investigate the influence of RPC and column size on punching shear capacity. Results showed that RPC in the drop panel increased punching shear capacity by 109%, with column dimensions significantly affecting shear resistance.

Keywords: Reactive Powder Concrete, Punching Shear, Flat Slabs, Drop Panel.

INTRODUCTION

The concrete and especially Reactive Powder Concrete (RPC) is a highly innovative and progressive form of construction material that has gained a lot of attention in the civil engineering sector of the modern world due to its superior mechanical properties. [1][2]. RPC is a type of ultra-high-performance concrete (UHPC), that is, with extremely low porosity and high strength. [3][4]. It is manufactured by the blending of ordinary Portland cement, silica fume, fine aggregates and the superplasticizers with or without addition of steel fibers. The final output of this piece is a material which is highly resistant to mechanical and environmental forces. [5][6]. The primary feature is that the RPC is capable of withstanding the punching shear failures, which characterize the flat slabs. An example of a failure situation that occurs in slabs during the course of the concentrated load, usually around the columns, is punching shear failure, where a localized failure occurs in the shape of a cone-shaped section being forced away out of the slab. It is a rather concerning type of failure, as it is unpredictable and deadly. Furthermore, the compressive strength of RPC is extremely high, and typically may range between 200 and 800 MPa; this allows a thinner slab to reduce the cost of the material and simplifies the construction process. Its resistance to high temperature is also very high which makes the material more versatile as far as its structural applications are concerned. This is what makes RPC the most optimal in the event of buildings that are exposed to adverse conditions such as fire resistant buildings. [9][10]. Reactive Powder Concrete (RPC) is far superior to normal concrete in regards to structures since it possesses superior mechanical and longevity properties. RPC possesses that characteristic, a depleted compressive strength, flexural strength, toughness, and low porosity, which makes it perform better compared to the high-performance concrete (HPC) and ordinary Portland cement (OPC) [11] [12].

This is a high-density granular packing RPC, and the incorporation of fine powders like silica fume leads to a high-ductile and low-permeability material [8] [9]. This material not only augments the fiber-matrix interfacial traits but also cannot be compared with tensile strain-hardening behavior; thus, RPC is the material of choice in those cases when the products are supposed to have a high level of durability and strength, like footbridges and structural repairs [13] [14]. Experimental research has also revealed that, at the expense of a 72 percent compressive strength increase, a 35.4 percent tensile strength increase, and a 38.2 percent modulus of elasticity increase when compared to normal concrete, RPC shows an increase in its compressive and tensile strength, respectively [13]. Also, its low porosity and resistance to chemical attacks and water infiltration make RPC have excellent durability; that is why it is applicable in the structure in the harsh environmental conditions [13] [14]. These properties not only ensure the increased durability of structures but also meet the requirements of sustainable development by decreasing the level of resource consumption and waste production [7]. In general, the best choice in RPC is that it is a more advanced

property that can be preferred in contemporary structural applications, and it holds innovations and developments in the construction industry [14] [15].

The objective of the present study is to investigate the punching shear improvement due to the replacement of normal concrete in the cross section by high-performance concrete (RPC) in the drop panel regain.

EXPERIMENTAL PART

Ordinary Portland Cement Type (I) AL -Mass production was employed in this study to make a concrete mix. All the cement was kept under controlled conditions to avoid the influence of humidity or atmospheric variations. The cement was tested chemically and physically based on the Iraqi specification (No. 5/2019) by the National Center of Construction Laboratories and Research, Kirkuk branch (NCCLR). The findings proved that the cement was of the required standards. Silica fume, which was the byproduct of silicon and ferrosilicon manufacturing, was included in the concrete mix. It is a fine material that is formed by heating fine quartz to silicon at elevated temperatures, which releases silicon oxide gases, which condense to create silica nanoparticles of non-crystalline nature. Silica fume can also be referred to as micro-silica, condensed silica fume, or silica dust. The American Concrete Institute (ACI) defines it as a very fine, non-crystalline byproduct, and it may contain pozzolanic and cementitious properties. Silica fume in this experiment is of a particle size of 0.1-1 μm, which is approximately 100 times smaller than cement particles. Silica fume is a good pozzolanic material for concrete because it contains high levels of SiO_2, fine particles, and has a high surface area. The silica fume employed in this experiment meets the physical and chemical regulations of the ASTM C1240-15. The fine aggregate of the concrete mix consisted of natural sand from the Qara Salem region. The fine aggregate is graded as below, and this is in line with the requirements of the Iraqi Specifications (IQS No. 45/2019). The physical characteristics of the fine aggregate are shown in the table. Fineness modulus, specific gravity, and absorption of the fine aggregate were ascertained in accordance with IQS No. 45/2019.

TABLE 1. Fine Sand Grading Compared with IQS No. 45/2019 Requirements

Sieve No.	Passing (%)	Limits of IQS No. 45/2019
3/8 in. (9.5 mm)	100	100
No. 4 (4.75 mm)	96.8	90–100
No. 8 (2.36 mm)	91.3	75–100
No. 16 (1.18 mm)	71.3	55–90
No. 30 (0.6 mm)	38.7	35 – 59
No. 50 (0.3 mm)	18.1	8 – 30
No. 100 (0.15 mm)	7.8	0 – 10

TABLE 2. Physical Properties of Fine Aggregate

Properties	Test Results	Specification
Dry Loose Unit Weight (kg/m³)	1644	ASTM C29/C29M – 17a
Materials Finer Than 0.075 mm	1.48	ASTM C117 – 17
Specific Gravity	2.69	ASTM C128–15
Absorption (%)	2.21	ASTM C128–15

The coarse aggregate used in the study was graded crushed gravel from Laylan fields, with a maximum size of 12.5 mm. The sieve analysis of the coarse aggregate is provided below, which meets the requirements of Iraqi Specifications (IQS No. 45/2019). The tests on this material were conducted at the University of Kirkuk, College of Engineering, Civil Engineering Department.

TABLE 3. Sieve Analysis of Coarse Aggregate

Sieve No.	Passing (%)	Limits of IQS No. 45/2019
3/4 in. (19 mm)	100	100
1/2 in. (12.5 mm)	100	100
3/8 in. (9.5 mm)	91.5	85–100
No. 4 (4.75 mm)	20.4	0 – 25
No. 8 (2.36 mm)	1.9	0 – 5

Master Glenium 51, a third-generation superplasticizer manufactured by BASF, was used to enhance the performance of the cement dispersion in the concrete mix. This superplasticizer reduces the amount of water required for the desired workability of the concrete. Unlike traditional superplasticizers, such as those based on melamine and naphthalene sulfonates, Master Glenium 51 is made from a polymer of long side-chain carboxylic ethers. This polymer initiates both electrostatic dispersion and steric hindrance, helping to achieve a highly flowable concrete mix with reduced water content. Master Glenium 51 complies with ASTM C494/C494M-2017 standards. Deformed steel 5 bars of Ø8 mm diameter in each direction were used for lateral reinforcement (drop panel reinforcement), and 10 mm diameter 15 bars in each direction were used for longitudinal reinforcement with two steel strain gauges for each sample at a distance of 150 mm from the center, represented as strain 2, and the other one at a distance of 150 mm from the edge of the sample, represented as strain 1. The mechanical properties of the steel reinforcement were determined using digital computerized testing tools, as shown in the table below. These steel bars comply with ASTM A615/615M-20 standards.

TABLE 4. Mechanical Properties of Steel Reinforcement

Diameter (mm)	Actual Diameter (mm)	Yield Stress (MPa)	Ultimate Strength (MPa)	Fu/Fy	Elongation (%)
8	8.94	323.87	543.16	0.68	6.1
10	9.78	581.32	644.7	1.11	10

RESULTS AND DISCUSSION

This study presents a comparison of the performance of four concrete specimens with different material types and configurations. The specimens consist of varying combinations of normal concrete (N.C.) and reactive powder concrete (R.P.C.) with uniform slab dimensions (940×940×60 mm) and drop panel dimensions (500×500×30 mm). Specimen C75-DN30: the slab and drop panel consist of normal concrete, the column size is 75 mm x 75mm and the compressive strength is 35.5 MPa. The specimen is used as a standard of the normal performance of concrete. Specimen C75-DR30: The slab is composed of normal concrete, and the drop panel is composed of R.P.C. The compressive strength of the slab is 45 Mpa and drop panel is 75 Mpa. This shows how R.P.C. has a high compressive strength and durability, particularly where it is most needed such as the drop panels that require additional weight. Specimen C125-DN30: Slab and drop panel are constructed of normal concrete, but the size of the column is enlarged to 125 mm × 125 mm forming a compressive strength of 39.3 MPa. The bigger column is characterized by a greater load bearing capacity with the type of concrete being the same. Specimen C125-DR30:

this specimen consists of a concrete slab that is normal and a panel of R.P.C drop. The slab strength is 32 Mpa whereas the drop panel is 75 Mpa. In spite of the reduced strength of slab being less than that of C125-DN30, R.P.C. drop panel makes up, providing sufficient overall structural strength. These results demonstrate the necessity of applying R.P.C. in such critical zones as drop panels where compressive strength is critical. They also note the critical importance of column dimensions in structural stability, but optimization of concrete material is essential in bringing about significant increment of compressive strength.

TABLE 5. Description of samples and main variables

NO	Specimen designation	Material	Column Dimension (mm)	Concrete Compressive Strength of Slab at 28 Days ($f'c$) (MPa)	Concrete Compressive Strength of Drop Panel at 28 Days ($f'c$) (MPa)
1	C75-DN30	Slab N.C, Drop Panel N.C	75 × 75	36	36
2	C75-DR30	Slab N.C, Drop Panel R.P.C	75 × 75	45	75
3	C125-DN30	Slab N.C, Drop Panel N.C	125 × 125	39	39
4	C125-DR30	Slab N.C, Drop Panel R.P.C	125 × 125	32	75

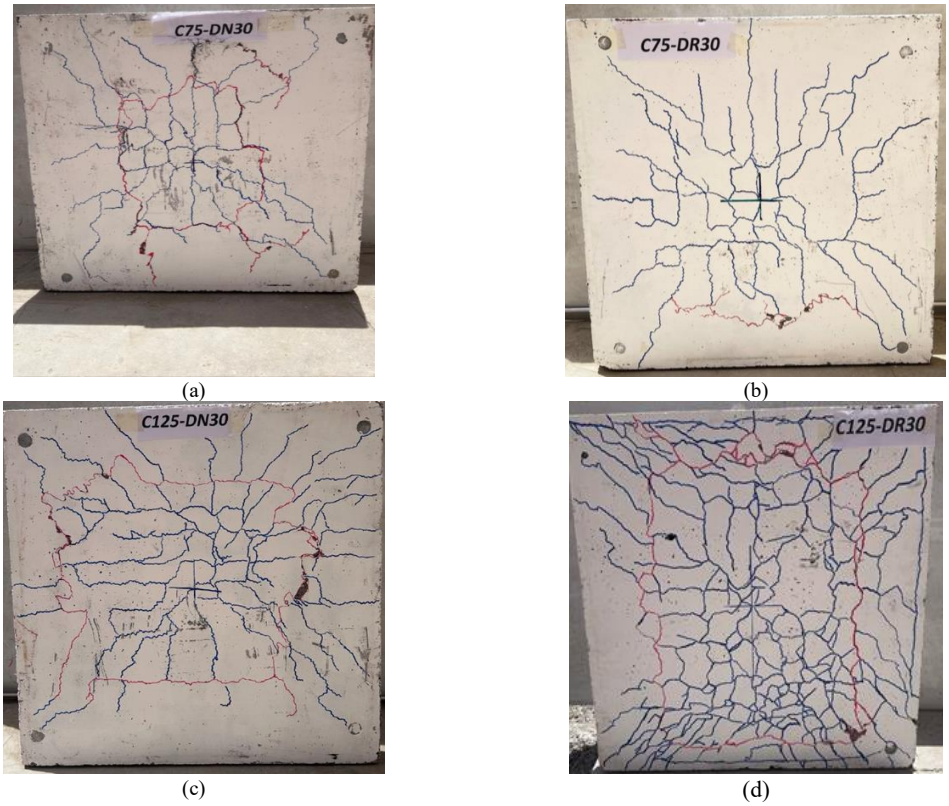

FIGURE 1. Shows the samples that are Shape a: Punching failure mode for specimen C75-DN30; Shape b: Mode of punching failure for specimen C75-DR30; Shape c: Mode of punching failure for specimen C125-DN30; and Shape d: Mode of punching failure for specimen C125-DR30.

The results presented in the figures provide a comprehensive analysis of the shear capacity and deformation behavior of different concrete specimens underloading. The following interpretation breaks down the findings, with references to the figures in the sequence they were provided. Figure 2 shows the load-deflection relationship for the four specimens, denoted as C75-DN30 (blue), C75-DR30 (orange), C125-DN30 (gray), and C125-DR30 (yellow). The x-axis of this figure shows the amount of deflection (in mm), whereas the y-axis shows the amount of load (in KN). Based on the graph, it can be observed that the specimens have varying load-bearing capacity and deflection properties. C75-DN30, according to the blue curve, shows the least load capacity. A maximum value was reached around 90 KN at a point of deflection of 3 mm. The C75-DR30 specimen (orange curve), in contrast, exhibits a higher peak load of 250 KN at around 6 mm of deflection of the material, which suggests a stiffer material response and is more able to withstand deformation due to applied load. Moreover, specimens C125-DN30 and C125-DR30, the two curves denoted as gray and yellow, respectively, have even higher loads on the peaks of 220 and 210 KN, respectively, and the deflections of the curves are at 7 mm and 8 mm, respectively. These findings are indicative of the fact that the C125 series, especially C125-DR30, exhibits a much greater shear capacity and load resistance than the C75 series, which means that the geometry of the specimen can influence performance.

Figure 2 A is narrowed down to the comparison of C75-DN30 (blue) and C75-DR30 (orange) specimens. The load-deflection curves of this figure indicate that C75-DR30 has a higher peak load and that the load attains a high value of about 230 KN at a deflection of 7 mm, whereas C75-DN30 attains a high value of 190 KN at a deflection of 5 mm. This can be interpreted to mean that the C75-DR30 specimen is stiffer and able to withstand deflection under comparable load conditions than the C75-DN30. The C75-DR30 sharper peak suggests that it has a greater resistance to deformation, and this could be explained by the material properties or, in this case, the reinforcement configuration of this specimen. Figure 2 B shows a comparison between C125-DN30 (gray) and C125-DR30 (yellow). The load-deflection curves depict that both specimens exhibit similar tendencies in terms of deflection, but C125-DR30 has a higher load capacity with a maximum load of 220 KN, as compared to C125-DN30, with the highest deflection of approximately 8 mm on both specimens. The findings indicate that shear capacity is high in the C125-DR30 when compared to C125-DN30, indicating that the DR30 in the C125 specimen is a stronger material response, maybe because of the reinforcement or the composition of the material. Figures 2 C and D shift focus to the load-strain relationships for C75-DN30, C75-DR30, C125-DN30, and C125-DR30 specimens. These figures plot the load (in KN) on the y-axis and strain (in mm/mm) on the x-axis, showing the elastic behavior of the reinforcement as it deforms under load. Figure 4 compares the strain response of C75-DN30 (blue and light blue) and C75-DR30 (orange and light orange). The curves show that both C75-DN30 and C75-DR30 exhibit linear elastic behavior in the initial loading stages, with load increasing proportionally to strain. However, C75-DR30 demonstrates a higher load response at a given strain, indicating a greater ability to resist deformation. This suggests that the material of C75-DR30 is more resistant to strain and exhibits enhanced load-bearing capacity. Similarly, Figure 5 shows the load-strain curves for C125-DN30 (gray and light gray) and C125-DR30 (yellow and light yellow). Again, the specimens display linear elastic behavior initially, with load increasing linearly with strain. However, C125-DR30 exhibits a higher load resistance for the same strain, reinforcing the observation from the load-deflection curves that C125-DR30 performs better under loading conditions. The difference between the strain responses of C125-DN30 and C125-DR30 further highlights the importance of reinforcement choices in determining the shear capacity and overall performance of these concrete specimens.

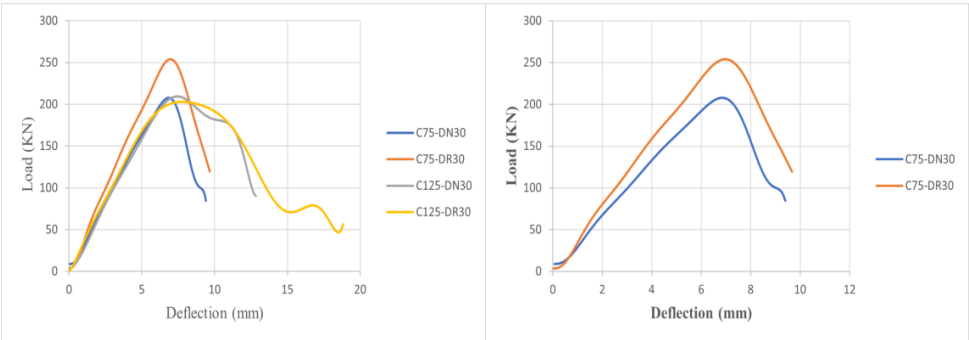

a b

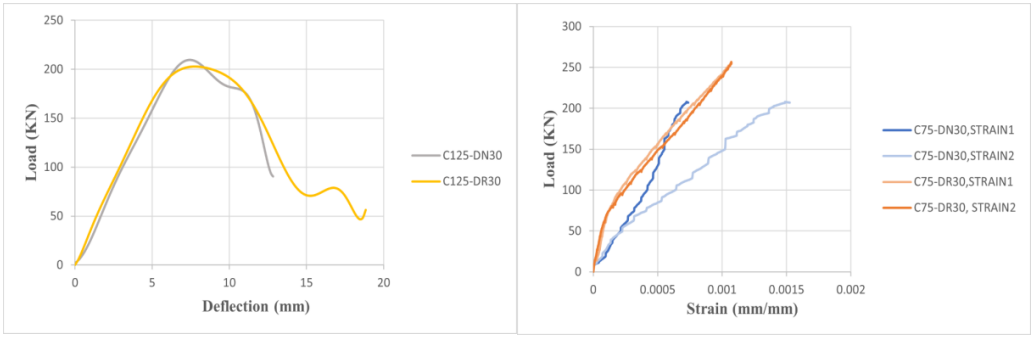

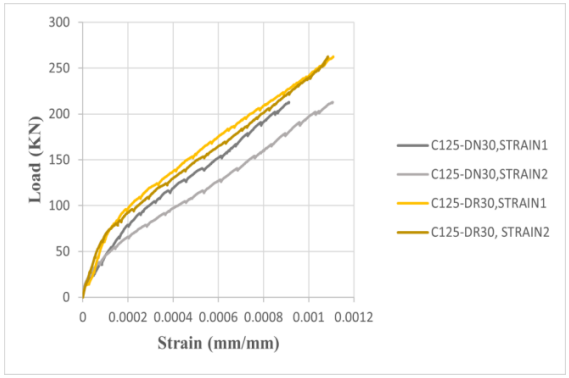

FIGURE 2. Shows a: Load-deflection curve for all specimens; b: Load-deflection comparison of (C75-DN30) and (C75-DR30); c: Load-deflection comparison of (C125-DN30) and (C125-DR30); d: Load-strain of steel comparison for (C75-DN30) and (C75-DR30); e: Load-strain of steel comparison for (C125-DN30) and (C125-DR30).

TABLE 6. Punching Shear Capacity Comparison: Analytical vs. Experimental Results

Specimen Name	ACI 318-19 (KN)	EC2 (KN)	Experimental Results (KN)
C75-DN30	88.52	98.30	207.85
C75-DR30	151.06	131.76	254.05
C125-DN30	124.13	118.02	209.53
C125-DR30	149.31	117.60	202.75

CONCLUSIONS

Four quarter-scale flat slab specimens with two different column sizes and concrete types within the drop panel area were tested under concentric load. The effect of RPC and column size on the punching shear capacity of concrete flat slabs was evaluated. The following conclusions could be drawn from this paper: Reactive Powder Concrete (RPC) is much better than Ordinary Concrete (OC) in diversified structural applications because it has superior mechanical and durability characteristics. RPC is superior in certain properties like high compressive and shear strength, which is ultra-high, has less porosity, and can withstand environmental and mechanical pressures and is therefore very appropriate in extreme condition structures. The comparative study indicates that the use of RPC in the drop panel section increases the punching shear capacity by 122% and 96% for slabs with column sizes of 75

mm and 125 mm, respectively, due to the increased concrete strength through the depth of the slab. Increasing the column size leads to an increase in the ultimate shear capacity of the slab by 100% and 80% for slabs with (N.C.) and (R.P.C.) drop panels, respectively.

REFERENCES

1. Oukaili, N. K. A., & Merie, H. D., "On the advantages in sustainability of structural concrete bubbled deck slabs," *IABSE Symp. Rep.*, 2019, pp. 1173-1181. doi: 10.2749/guimaraes.2019.1173.
2. Oukaili, N., Merie, H., Allawi, A., & Wardeh, G., "Reduced volume approach to evaluate biaxial bubbled slabs' resistance to punching shear," *Build.*, 14(3), 676, Mar. 2024. doi: 10.3390/buildings14030676.
3. Oukaili, N. K. A., & Merie, H. D., "Reduction of shear resistance in bubble decks with openings," *Conf. Paper*, Oct. 2018. Available: https://www.researchgate.net/publication/328412221.
4. Oukaili, N. K. A., & Merie, H. D., "Sustainability analysis and shear capacity of bubble deck slabs with openings," *Conf. Paper*, Sept. 2018. doi: 10.1109/DeSE.2018.00051.
5. Hassan, F. H., & Sarsam, K. F., "Punching shear failure characteristics of flat slabs using reactive and modified powder concrete with steel fibers," *J. Eng. Dev.*, 17(5), 124-129, Nov. 2013.
6. Chassib, S. M., "Punching shear strength of reactive powder concrete slabs reinforced with CFRP bars," Ph.D. thesis, Civil Eng. Dept., Univ. of Baghdad, Baghdad, Iraq, 2016.
7. Baniya, W. J., et al., "Behavior of composite pre-flat slabs in resisting punching shear forces," *Alex. Eng. J.*, 59, 333-347, 2020. doi: 10.1016/j.aej.2019.12.045.
8. Abdurrahman, M. B., & Hussein, A. A., "Punching strength of reactive powder reinforced concrete flat slabs," *Tikrit J. Eng. Sci.*, 28(3), 35-47, 2021.
9. Ali, Y. S., Warsh, W. A., & Yousif, M. A., "Increasing ultimate strength of reinforced concrete slab by using reactive powder concrete and study the effect of high temperature on them," *Anbar J. Eng. Sci.*, 8, 16-26, 2019.
10. Atea, R. S., Dheyab, H. M., & Aljazaari, R. A., "Punching shear of reinforced concrete slabs bonded with reactive powder after exposure to fire," *Open Eng.*, 13, 1-6, 2023. doi: 10.1515/eng-2022-0393.
11. Sanjuán, M. Á., & Andrade, C., "Reactive powder concrete: Durability and applications," *Appl. Sci.*, 11(12), 5629, 2021. doi: 10.3390/APP11125629.
12. Sahani, B. S., & Ray, N. H. S., "A comparative study of reactive powder concrete and ordinary Portland cement by ultra-high strength technology," *Int. J. Res.*, 1(6), 524-534, 2014.
13. Jaafar, A., Azeez, A. A., Hassen, D. R., & Yussof, M. M., "An experimental investigation into the characteristics and performance of reactive powder concrete to choose the ideal mix," *BIO Web Conf.*, 2024, art. no. 970094. doi: 10.1051/bioconf/20249700094.
14. Zhao, Y., "Performance analysis and application fields of reactive powder concrete," *Appl. Comput. Eng.*, 63, 2024. doi: 10.54254/2755-2721/63/20241009.
15. Roux, N., Andrade, C., & Sanjuán, M. Á., "Experimental study of durability of reactive powder concretes," *J. Mater. Civ. Eng.*, 8(1), 1-6, 1996. doi: 10.1061/(ASCE)0899-1561(1996)8:1(1).